

Three-dimensional characterization of collagen remodeling in cell-seeded collagen scaffolds via polarization second harmonic generation: supplement

DIONYSIOS XYDIAS,^{1,2} GEORGIOS ZIAKAS,² SOTIRIS
PSILODIMITRAKOPOULOS,¹ ANDREAS LEMONIS,¹ ELENI BAGLI,³
THEODORE FOTSIS,³ ACHILLE GRAVANIS,^{4,5} DIMITRIOS S.
TZERANIS,^{4,6} AND EMMANUEL STRATAKIS^{1,7,*} 

¹*Institute of Electronic Structure and Laser, Foundation for Research and Technology-Hellas, Greece*

²*Department of Materials Science and Technology, School of Sciences and Engineering, University of Crete, Greece*

³*Department of Biomedical Research, Institute of Molecular Biology and Biotechnology, Foundation for Research and Technology-Hellas, Ioannina, Greece*

⁴*Institute of Molecular Biology and Biotechnology, Foundation for Research and Technology-Hellas, Greece*

⁵*Department of Pharmacology, School of Medicine, University of Crete, Greece*

⁶*Department of Mechanical and Manufacturing Engineering, University of Cyprus, Cyprus, Greece*

⁷*Department of Physics, School of Sciences and Engineering, University of Crete, Greece*

*stratak@iesl.forth.gr

This supplement published with The Optical Society on 28 January 2021 by The Authors under the terms of the [Creative Commons Attribution 4.0 License](https://creativecommons.org/licenses/by/4.0/) in the format provided by the authors and unedited. Further distribution of this work must maintain attribution to the author(s) and the published article's title, journal citation, and DOI.

Supplement DOI: <https://doi.org/10.6084/m9.figshare.13315904>

Parent Article DOI: <https://doi.org/10.1364/BOE.411501>

3D Characterization of Collagen Remodeling in Cell-seeded Collagen Scaffolds via Polarization Second Harmonic Generation

DIONYSIOS XYDIAS,^{1,2} GEORGIOS ZIAKAS,² SOTIRIS PSILODIMITRAKOPOULOS,¹ ANDREAS LEMONIS,¹ ELENI BAGLI,³ THEODORE FOTSIS,³ ACHILLE GRAVANIS,^{4,5} DIMITRIOS S. TZERANIS,^{4,6} AND EMMANUEL STRATAKIS,^{1,7,*}

¹*Institute of Electronic Structure and Laser, Foundation for Research and Technology-Hellas, Greece*

²*Department of Materials Science and Technology, School of Sciences and Engineering, University of Crete, Greece*

³*Department of Biomedical Research, Institute of Molecular Biology and Biotechnology, Foundation for Research and Technology-Hellas, Ioannina, Greece*

⁴*Institute of Molecular Biology and Biotechnology, Foundation for Research and Technology-Hellas, Greece*

⁵*Department of Pharmacology, School of Medicine, University of Crete, Greece*

⁶*Department of Mechanical and Manufacturing Engineering, University of Cyprus, Cyprus*

⁷*Department of Physics, School of Sciences and Engineering, University of Crete, Greece*

*stratak@iesl.forth.gr

© 2020 Optical Society of America under the terms of the [OSA Open Access Publishing Agreement](#)

Supplementary material

S.1 Imaging setup

The beam after the galvanometric mirrors is focused in a single diffraction-limited spot on the sample plane, the sample is excited and the emitted light is collected in one or more Photon Multiplier Tubes (PMTs) (H9305-04, Hamamatsu, Hizuoka, Japan), depending on our choice of reflective in the turret box and recorded using a custom LabView module. Moving the galvanometric mirrors translates the position of the spot on the sample plane in x and y axes. Thus, with a synchronized movement of the mirrors, an entire region of the sample is scanned and we acquire an image of the sample with a field of view depending on the voltage amplitude supplied to the galvanometric mirrors.

Light reaching the PMTs is filtered by a combination of a short-pass filter at 680 nm (FF01-680/SP, Semrock) and a band-pass filter suitable for each individual signal. For the forwards detection, which we use for the SHG signal, we installed a narrow 514/3 filter (FF01-514/3, Semrock). For the backwards detection, which we use to collect the signals originated from the various fluorescent dyes, we have 3D-printed an adaptor-base which allows for separation and detection of the individual MPEF signals, see figure (4). In its entrance, a 680SP filter blocks the source light and we use a long-pass dichroic mirror (509-FDi01, Semrock) placed at 45°, to split the incoming beam into two perpendicular parts. The reflected part (smaller wavelengths) is filtered by a 458/64 band-pass filter (FF1-458/64, Semrock) and the transmitted by a 527/20 band-pass filter (FF01-527/20, Semrock), to match the emissions of the fluorescent dyes used, Hoechst and Calcein, respectively.

Fig. S1 shows an overlap of the absorption (left) /emission (right) spectra of the fluorescent dyes and collagen together with vertical lines for the dichroic and the various filters used, to visualize how the combination of the filters described in methods is suitable for the isolation of each signal. Fluorescence data for this plot were acquired from <http://thermofisher.com/>.

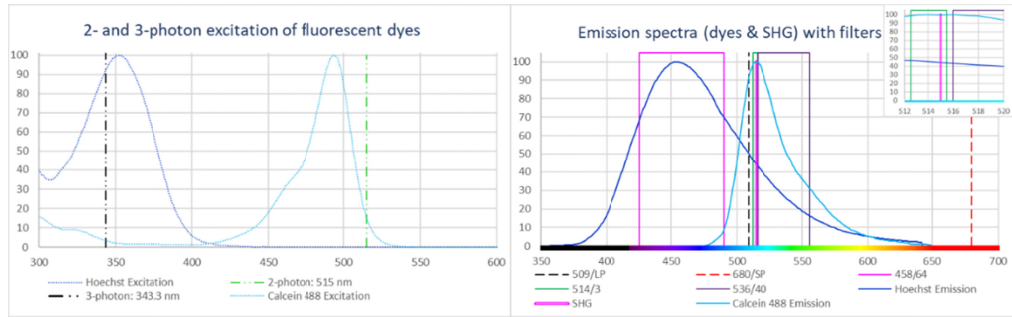


Fig. S1. Left: Absorption spectra of Hoechst and CalceinAM superimposed on utilized lines for 2- or 3-photon excitation. Right: Emission spectra of Hoechst and CalceinAM superimposed on the detection spectral regions of the three PMTs utilized. The inset shows in detail the separation of collagen SHG and CalceinAM fluorescence in the region 512 – 520 nm.

S.2 PSHG directionality in collagen-based scaffolds

SHG directionality in collagen scaffolds depends on whether the scaffolds are dry or wet. In dry scaffolds, the majority of the SHG signal was detected backwards, while for wet scaffold the majority of the SHG signal was detected in the forward collection geometry.

In Fig S2 we present a comparison of the strength of collagen SHG signal, for a single polarization orientation, between forward and backward detection for both the cases of dry and wet scaffolds. On the top row, we show our results for collagen, while on the bottom row the scaffold was wet.

We observe that in the case of dry scaffolds, the signal is much stronger in the backwards direction, while this changes when the scaffold is wet. Since all live samples are wet, this means that in our triple PMT setup, it is much preferable to detect collagen SHG in the forwards direction, as described in the methods in the main text.

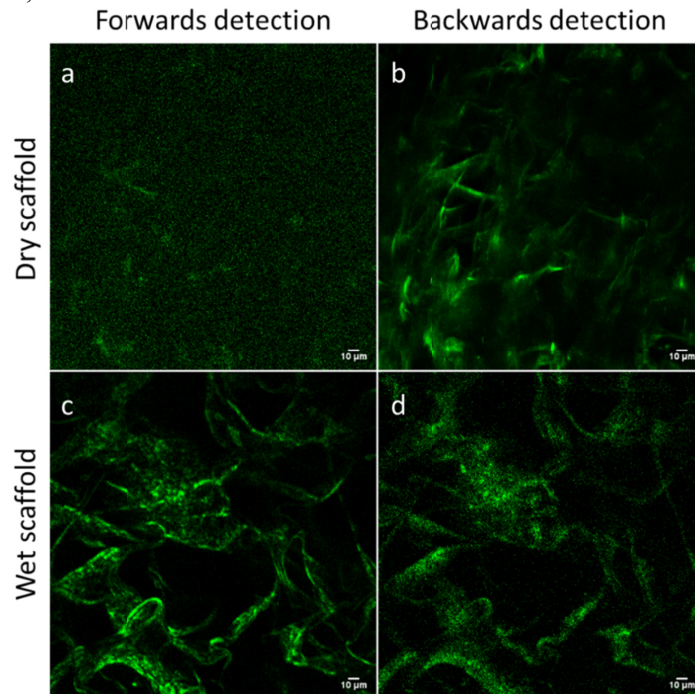


Fig. S2. Comparison of SHG signal strength in the forwards and backwards direction for dry and wet CGS. For dry samples(a,b) the signal is stronger in the backwards direction, while the opposite is true for wet scaffolds (c-d).

S.3 Volume statistics

CGS areas were defined by selecting pixels with intensities above a threshold of 5% of max signal in the SHG channel (514/3 nm), that shows only the SHG from the collagen fibers (green in Fig. 4(a)). For cell areas, the two fluorescence channels of our microscope (485/64 nm (blue) and 536/40 nm (red)), both depicting cellular mass, were initially combined in one image, using the logical OR function in ImageJ. Then a 5% threshold was applied. Finally, we calculated % Areas, by dividing the corresponding pixel numbers by the total area of each image, i.e. 500x500 pixels = 250000 pixels. Finally, we calculated the cellular center of mass inside each scaffold using the cell % Area as a weight.

Fig. S3 shows plots of area fraction occupied by cells (orange) and collagen (blue) versus the depth of the scaffold, at each DIV. The criterion used here for maximum depth penetration was set to the percentage of the cellular area in each image dropping to less than 1%. At 3 DIV cells can be found at a maximum depth of 48 μm inside the scaffold and collagen comprises a bigger fraction of each area than cells. At 5 DIV the maximum penetration of cells has only slightly changed to 52 μm and a wider spread of cells was observed towards the exterior. At 7 DIV, cells occupy a larger fraction of the area than collagen, an effect much more noticeable at 10 DIV. The maximum cell penetration at 7 and 10 DIV is 72 μm and at least 100 μm respectively.

The diameter of CGS collagen fibers was analyzed using the DiameterJ (version 1-017) plugin of ImageJ (version 1.48v). DiameterJ automatically detects all fibers in a 2D image and determines their diameters, based on user-defined thresholds that best match the initial image. We repeated this procedure for all the layers of the acquired z-stacks. Fig. S5 shows the resulting average collagen fiber diameter for each layer and sample studied. Results show that control cell-free CGS have thicker fibers than cell-seeded CGS. Reported diameter values for each sample in the main text are averages over all z-planes shown in Fig. S4.

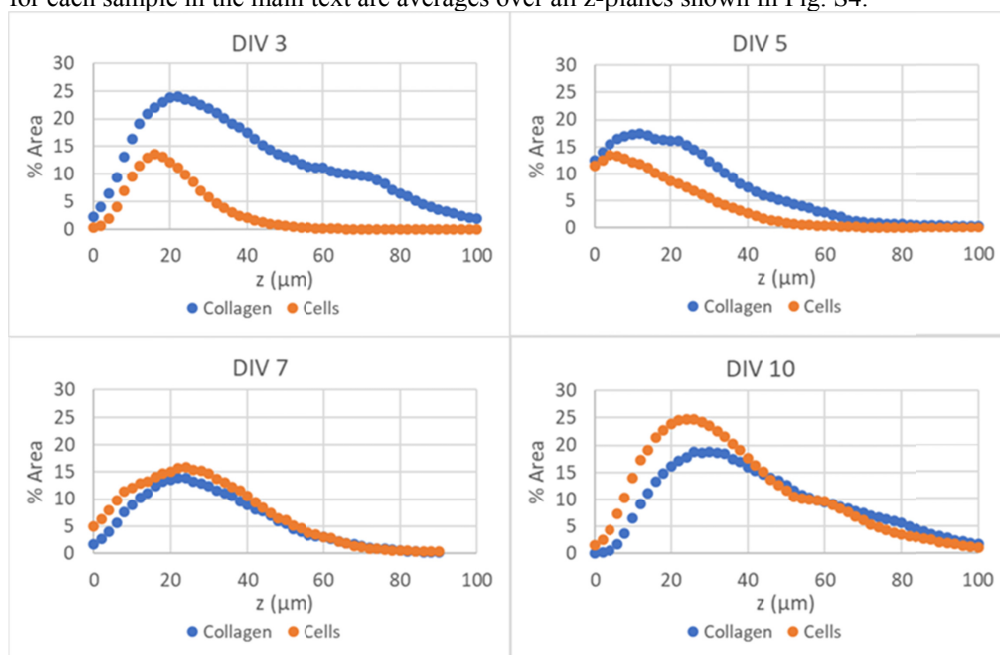


Fig. S3. Fraction of cells and collagen areas inside the scaffold for every z-plane inside CGS. Maximum cell penetration inside CGS progressively increase from 50 μm at 3 DIV to least 100 μm at 10 DIV.

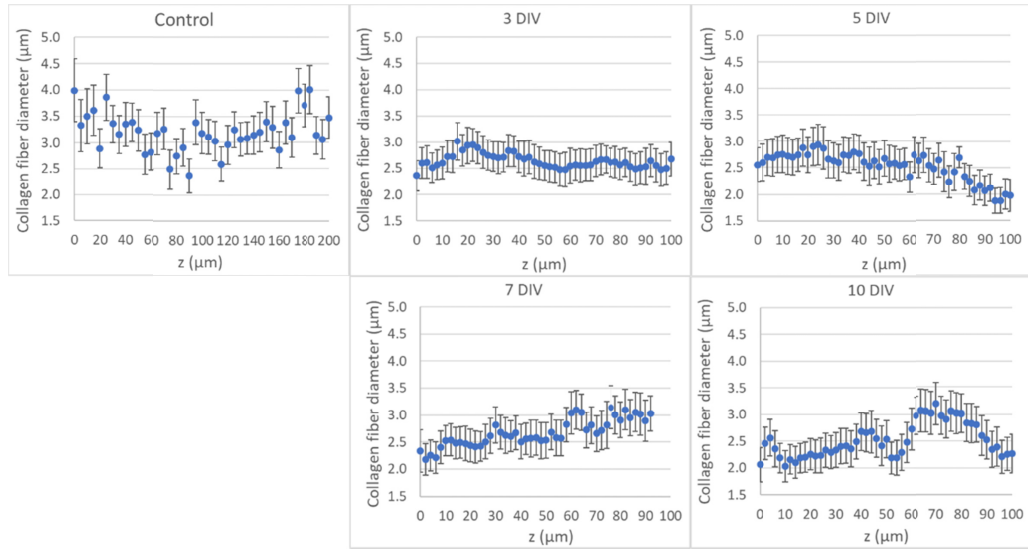


Fig. S4. Plots of CGS fiber diameter as a function of z-depth for control and cell-seeded CGS. Data are presented as mean \pm s.e.m.